

Article

# Design and Fabrication of a Holographic Radial Polarization Converter

Jing-Heng Chen <sup>1,\*</sup>, Hung-Lung Tseng <sup>1</sup>, Fan-Hsi Hsu <sup>2</sup>, Chien-Yuan Han <sup>3</sup>, Kun-Huang Chen <sup>4</sup>, Chien-Hung Yeh <sup>1</sup> and Ken-Yuh Hsu <sup>5</sup>

<sup>1</sup> Department of Photonics, Feng Chia University, No. 100, Wenhwa Rd., Seatwen, Taichung 40724, Taiwan; m0823516@o365.fcu.edu.tw (H.-L.T.); yehch@fcu.edu.tw (C.-H.Y.)

<sup>2</sup> Center for Measurement Standards, Industrial Technology Research Institute, No. 321, Sec. 2, Kuang Fu Rd., Hsinchu 30011, Taiwan; FHHsu@itri.org.tw

<sup>3</sup> Department of Electro-Optical Engineering, National United University, No. 2, Lienda, Nanshi Li, Miaoli 36063, Taiwan; cyhan@nuu.edu.tw

<sup>4</sup> Department of Electrical Engineering, Feng Chia University, No. 100, Wenhwa Rd., Seatwen, Taichung 40724, Taiwan; chenkh@fcu.edu.tw

<sup>5</sup> Department of Photonics, College of Electrical and Computer Engineering, National Chiao Tung University, 1001 University Road, Hsinchu 30010, Taiwan; ken@cc.nctu.edu.tw

\* Correspondence: jhchen@fcu.edu.tw

Received: 29 August 2020; Accepted: 28 September 2020; Published: 1 October 2020



**Abstract:** Radial polarization converters can convert an incident light into a radially polarized light, which is beneficial in a variety of applications. In this paper, a new design of holographic radial polarization converter is proposed which consists of eight space-variant polarization-selective volume hologram gratings. According to the coupled wave theory, a feasible design of the polarization-selective volume hologram gratings was described. The prism-hologram-prism sandwiched recording method was adopted for the recording. The *s*- and *p*-polarization diffraction efficiencies of the fabricated polarization-selective volume hologram gratings at 443.29 nm are 90.83% and 22.09%, respectively. The operation bandwidth is about 4.42 nm. A prototype of holographic radial polarization converter was successfully assembled and tested. Due to the introduction of volume hologram gratings, this design should have the advantages of high diffraction efficiency, narrow band, compactness, and planar configuration, meaning it is especially suitable for low-cost mass production and has high application potential in related fields.

**Keywords:** coupled wave theory; radial polarization; holographic optical elements; volume gratings; polarization-selective devices

## 1. Introduction

Radial polarization converters (RPCs) are capable of converting a linearly, circularly, or un-polarized light into radially and azimuthally polarized lights which have a variety of applications, such as high-resolution microscopy, surface plasmon excitation, optical trapping, material processing, light actuating materials, and high-density data storage [1–6]. Several methods have been proposed for the generation of radially and azimuthally polarized lights, which can be categorized as intra-cavity and extra-cavity methods. For the intra-cavity method, two orthogonal Hermite–Gaussian TEM<sub>10</sub> and TEM<sub>01</sub> modes are generated and superimposed inside the laser cavity to obtain the output of radially and azimuthally polarized lights. Some special designed elements, such as birefringent crystal, adjustable aperture, axicon, or non-periodic sub-wavelength gratings, are set inside the laser cavity for this purpose [7,8]. Due to the complexity of the cavity, the method suffers from the difficulties of alignment and additional power losses in laser manufacturing. In addition, limited by the form of

laser cavity, the intra-cavity method is not suitable for fiber lasers, lithography ultraviolet (UV) lasers, or semiconductor lasers. For the extra-cavity method, it can also be divided into two types of technique. The first type of technique, similar to the intra-cavity method, uses various interferometric structures to generate and superimpose two orthogonal Hermite–Gaussian TEM<sub>10</sub> and TEM<sub>01</sub> modes outside the laser cavity [9–11]. Therefore, this technique has high requirements for the coherence of the light source and the stability of the environment and has relatively lower power. The second type of technique uses a variety of specially designed elements, such as space-variant half-wave plates, sub-wavelength metal stripe gratings, liquid-crystal elements, dielectric metasurfaces, and waveguide gratings, to convert a linearly or circularly polarized light into radially and azimuthally polarized lights [2,12–16]. Nowadays, various commercial radial polarization converters are available. However, they may not be easy to manufacture, and therefore the cost is relatively high. By contrast, volume hologram gratings can be an alternative feasible solution for the radial polarization converter, which provide superior characteristics of high diffraction efficiency, thin and compact plane configuration, easy coupling of light, low cost, and are suitable for mass production. In recent decades, although volume hologram gratings have been successfully applied, the challenge of new applications still lies in the design and practical recording method [17,18]. According to the author’s knowledge, no holographic radial polarization converters have been proposed. In 2018, our research group had proposed a new prism-hologram-prism sandwiched recording method for the recording of polarization-selective substrate-mode volume holograms with a large diffraction angle which can be applied [18].

Therefore, in this paper, a new design of holographic radial polarization converter (HRPC) is proposed for the first time. The proposed HRPC consists of eight space-variant cut polarization-selective volume hologram gratings (PVHG). According to the coupled wave theory, the design-related parameters and manufacturing considerations of the PVHGs are described. The prism-hologram-prism sandwiched holographic recording method was adopted for the practical fabrication of PVHGs. The *s*- and *p*-polarization diffraction efficiencies of the fabricated PVHGs at 443.29 nm are 90.83% and 22.09%, respectively. With the fabricated PVHGs, a prototype HRPC was assembled and tested. The results successfully verify that the holographic radial polarization converter does have the characteristics of radial polarization. Due to the introduction of volume hologram gratings, this new element should have advantages of most holographic optical elements, meaning that it especially suitable for low-cost mass production and has high application potential in related fields.

## 2. Principles

The structure and operating principle of the proposed polarization-selective volume hologram gratings (PVHG) is depicted in Figure 1. The PVHG is attached to a substrate and covered with a coversheet. For ease of understanding, an *r*-*z* orthogonal coordinate system is introduced. When an un-polarized light is incident on the PVHG perpendicularly along the *z*-axis, either *s*- or *p*-polarized light is diffracted completely by the PVHG into the coversheet with multiple total internal reflections along the *r*-axis direction. Therefore, the incident plane lies in the *r*-*z* coordinate plane. The other polarized light is forward-transmitted through the coversheet. In this case, according to the coupled wave theory, the diffraction efficiencies of *s*- and *p*-polarization can be written as [17,19]:

$$\eta_s = \sin^2 v_s = \sin^2 \left[ \frac{\pi n_1 d}{\lambda_2 (\cos \theta_d)^{1/2}} \right] = \sin^2 \left[ \frac{\pi N_1}{(\cos \theta_d)^{1/2}} \right], \quad (1)$$

$$\eta_p = \sin^2 v_p = \sin^2 (v_s \cos \theta_d), \quad (2)$$

where the subscripts *s* and *p* represent *s*- and *p*-polarization,  $\theta_d$  is the diffraction angle in the PVHG,  $v_s$  and  $v_p$  are the modulation parameters,  $n_1$  is the refractive index modulation,  $d$  is the thickness of hologram emulsion,  $\lambda_2$  is the wavelength of reconstruction light, and  $N_1 = n_1 d / \lambda_2$  is the effective refractive modulation. Obviously, the diffraction efficiencies of *s*-polarization and *p*-polarization are two sine square functions with asynchronous oscillations. Consequently, as shown in Figure 2a–c,

the feasible diffraction angles that satisfy the aforementioned functions of PVHG exist at  $48.19^\circ$ ,  $60^\circ$ , and at a large angle around  $85^\circ$ , and the required values of effective refractive modulation  $N_1$  are 1.22, 0.71, and 0.15. Under these conditions, the corresponding diffraction efficiencies ( $\eta_s, \eta_p$ ) are (100%, 0%) at  $48.19^\circ$ , (0%, 100%) at  $60^\circ$ , and (100%, 1.93%) around  $85^\circ$ . Limited by the finite strength of phase modulation  $n_1d$  of recording material, a smaller effective refractive modulation  $N_1$  is easier to implement for a specified reconstruction wavelength.

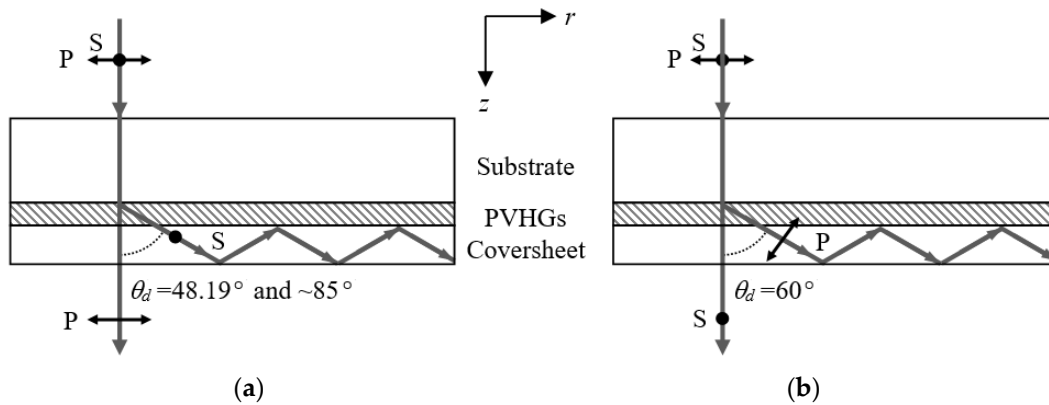


**Figure 1.** Structure and operating characteristics of polarization-selective volume hologram gratings (PVHGs) designed at (a)  $\theta_d = 48.19^\circ$  and  $\sim 85^\circ$ , and (b)  $\theta_d = 60^\circ$ .

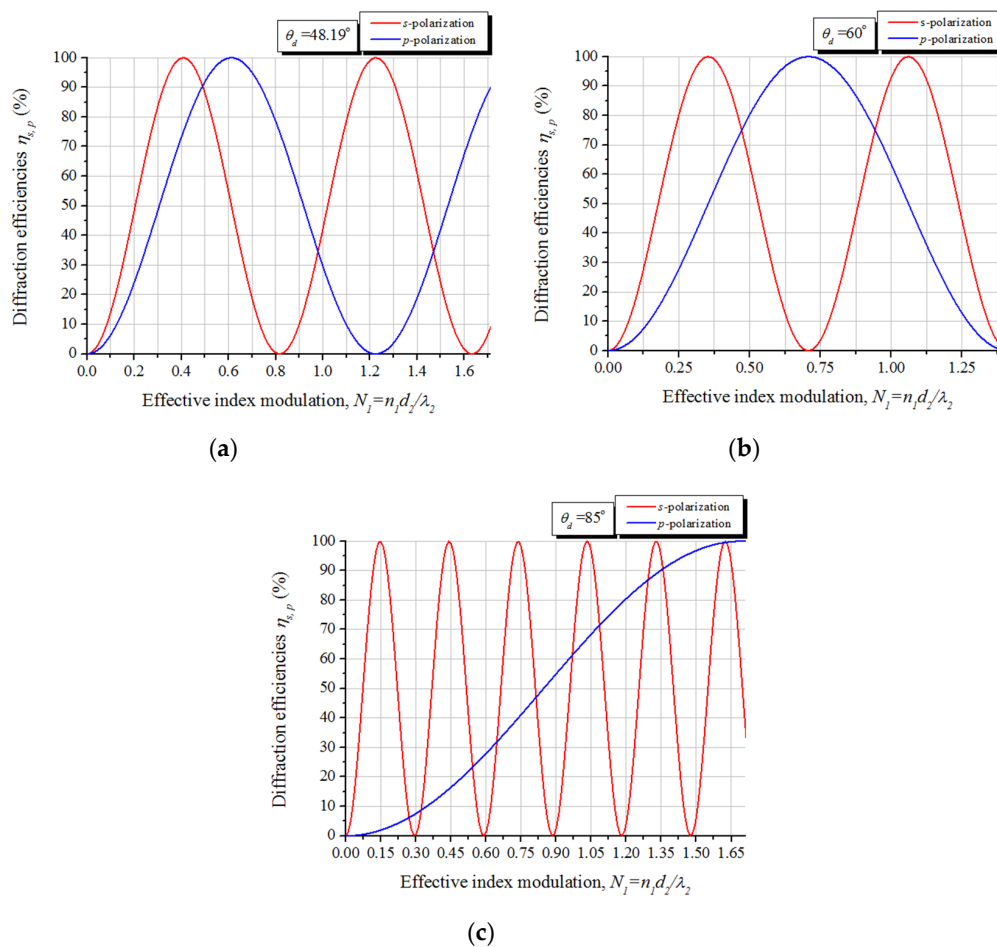


**Figure 2.** Diffraction efficiencies versus effective index modulation at (a)  $\theta_d = 48.19^\circ$ ; (b)  $\theta_d = 60^\circ$ ; (c)  $\theta_d = 85^\circ$ .

Accordingly, the architectures and operating principles of the proposed holographic radial and azimuthal polarization converters can be depicted in Figure 3, which consist of a radially symmetrical distribution of eight fan-shaped cut sub-PVHGs with its incident plane ( $r$ - $z$  coordinate plane) aligned in radial directions. As shown in Figure 3a, a holographic radial polarization converter (HRPC) can be achieved when the diffraction angle and effective refractive modulation ( $\theta_d, N_1$ ) are designed at  $(48.19^\circ, 1.22)$  and around  $(85^\circ, 0.15)$ . In Figure 3b, a holographic azimuthal polarization converter (HAPC) can be achieved when the diffraction angle and effective refractive modulation ( $\theta_d, N_1$ ) are designed at  $(60^\circ, 0.71)$ . However, radial polarization converters are more preferred and applicable in practical applications.

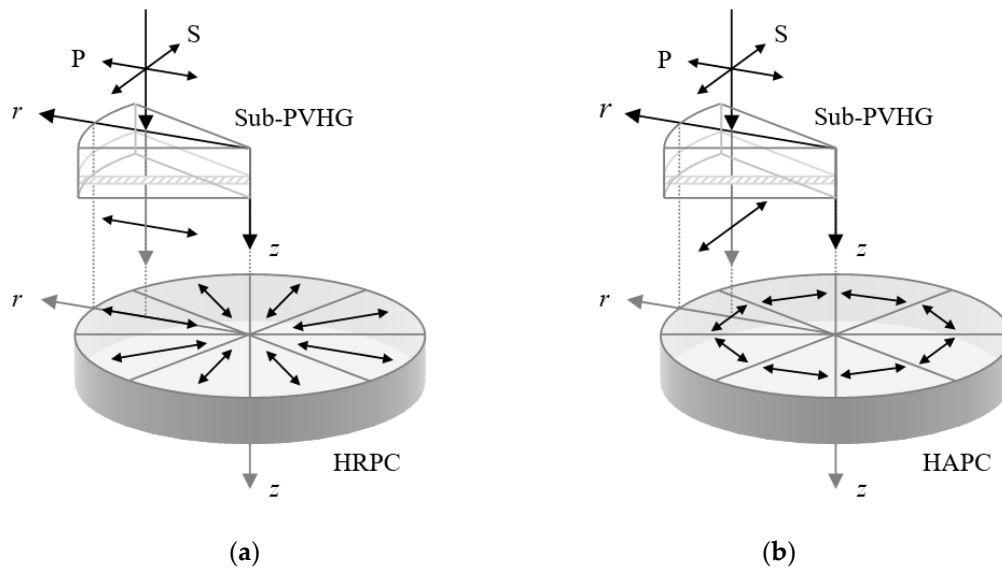


**Figure 3.** Structure and operating characteristics of (a) a holographic radial polarization converter (HRPC) and (b) a holographic azimuthal polarization converter (HAPC).

### 3. Experimental Results and Discussions

In order to verify the feasibility of this design, a prototype holographic radial polarization converter (HRPC) was assembled and tested. Firstly, the polarization-selective volume hologram gratings (PVHGs) were recorded with photopolymer film (C-RT20, Litiholo) ( $n_{pp} = 1.501$ ,  $d = 16 \mu\text{m}$ ) with a 632.8 nm He-Ne laser. As shown in Figure 4, a prism-hologram-prism sandwiched recording setup was adopted for the recording [18]. In fabrication, the photopolymer film was sandwiched between two right-angle prisms with a base angle  $\theta_{p1}$  of  $45^\circ$  for recording. The collimated incident and reflected laser beams were served as a reference beam and object beam, respectively. Then, the fabricated PVHG was cut into eight sub-PVHGs with an isosceles triangle shape which were used to assemble the prototype of HRPC, as shown in Figure 5. The dimensions of base  $\times$  height of each sub-PVHG were approximately  $5.0 \times 6.0$  mm, and the diameter of the assembled HRPC was about 12 mm. The fabricated PVHG and assembled HRPC were tested with a linearly polarization-controlled tungsten halogen white-light source (HL-2000, Ocean Optics), as shown in Figure 6. As displayed in Figure 6a, combined with spectrometer (HR4000CG-UV-NIR, Ocean Optics), the polarization-controlled spectrum intensities with and without PVHG were measured. Then, as shown in Figure 7, the spectrum diffraction efficiencies for  $s$ - and  $p$ -polarizations at a central wavelength of 443.29 nm were determined with values of 90.83% and 22.09%, respectively, which confirmed the polarization-selective function of the PVHG. The theoretical central wavelength and diffraction angle should be 443.6 nm and  $83.54^\circ$ , respectively. The measured bandwidth of  $s$ -polarization light with diffraction efficiency of 80% is about 4.42 nm. In the insets of Figure 7, the PVHG has a purple appearance corresponding with the wavelength of 443.29 nm, when  $s$ -polarized light is incident. This is due to the scattering phenomenon

caused by multiple total internal reflections of the *s*-polarized diffracted light in the polycarbonate coversheet ( $n_{pc} = 1.608$ ,  $d_{pc} = 180 \mu\text{m}$ ). Meanwhile, the PVHG has a white appearance when *p*-polarized light is incident.

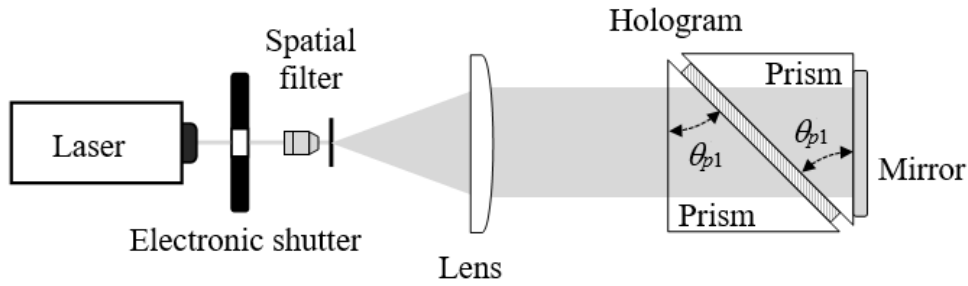


Figure 4. Prism-hologram-prism sandwiched recording setup.

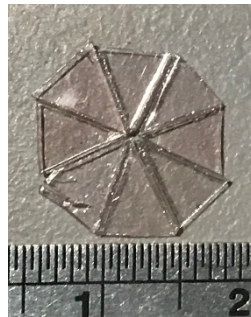


Figure 5. A prototype of holographic radial polarization converter (HRPC).

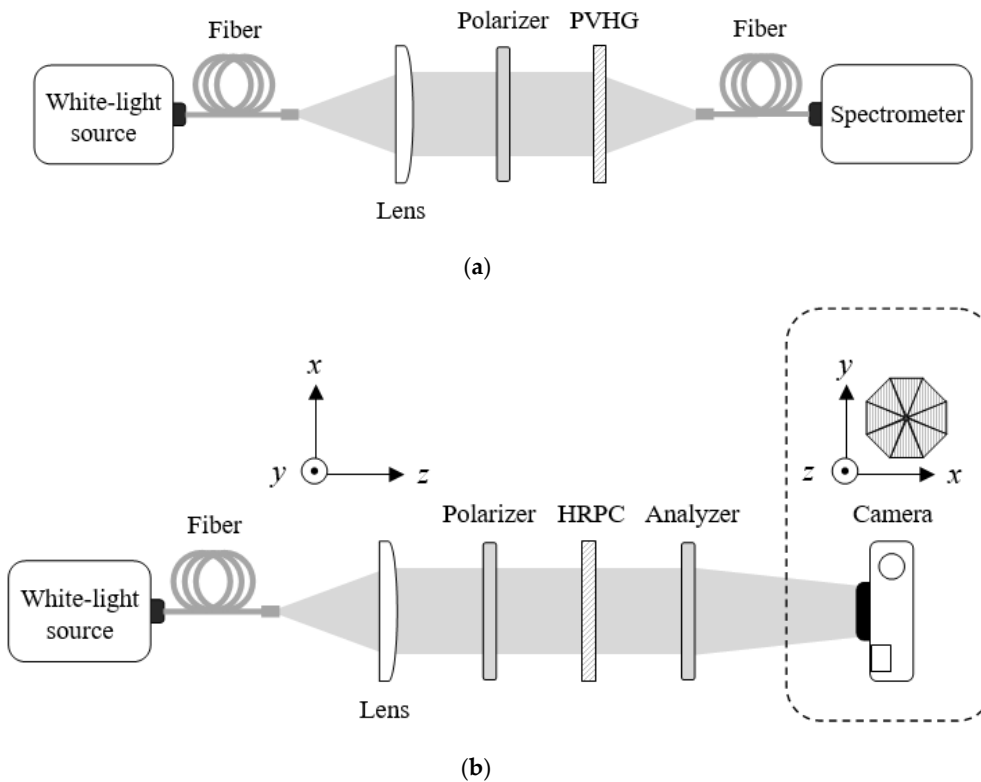
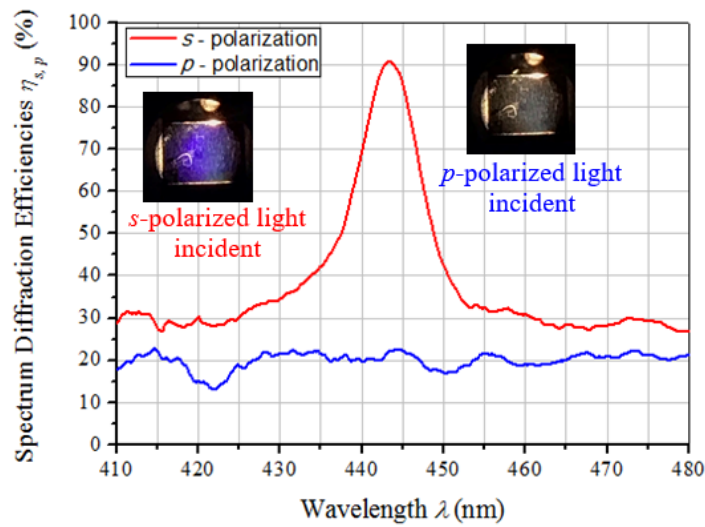
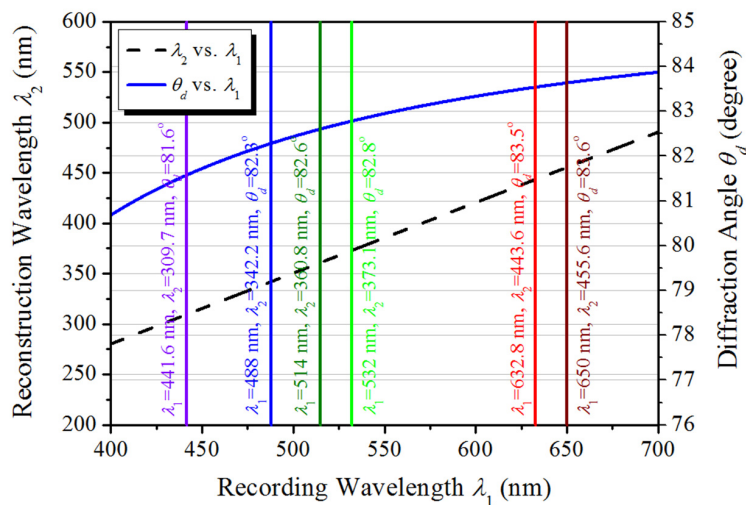


Figure 6. Polarization controlled white-light source testing system for the measurement of (a) spectrum diffraction efficiencies; (b) light field distributions.



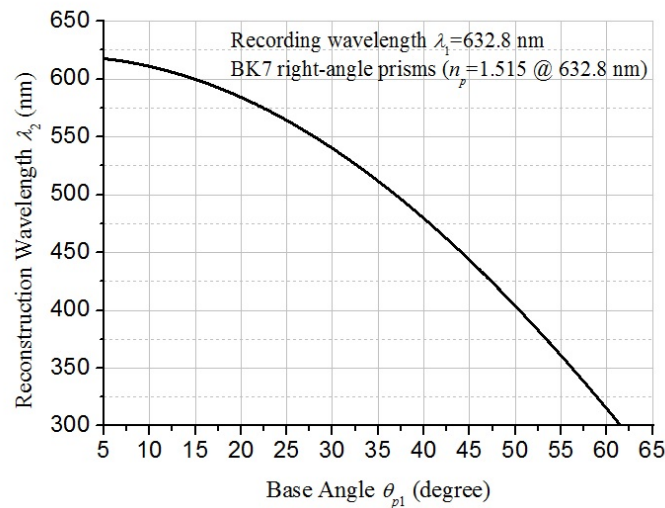
**Figure 7.** Spectrum diffraction efficiencies for *s*- and *p*-polarizations and appearances with *s*- and *p*-polarized incident lights.

According to the geometry of prism-hologram-prism sandwiched recording setup, the reconstruction wavelength  $\lambda_2$  (operating wavelength) can be tuned by changing the recording wavelength  $\lambda_1$  or the base angle  $\theta_{p1}$  of applied right-angle prisms [18]. In Figure 8a, the relationship of reconstruction wavelength  $\lambda_2$  versus recording wavelength  $\lambda_1$  is depicted with relevant thickness and refractive index parameters. Considering the most commonly used commercial lasers for holography, the corresponding wavelengths are marked and summarized in Table 1. In addition, the corresponding diffraction angles  $\theta_d$  are all above  $81^\circ$ , which can meet the requirement of a large angle in the design. In addition, different from the traditional holographic recording method, this method belongs to a technique of longer wavelength construction for shorter wavelength reconstruction. As shown in Figure 8b, considering a specific recording wavelength of 632.8 nm, the reconstruction wavelength  $\lambda_2$  (operating wavelength) can be continuously tuned from 300.05 nm to 617.73 nm when the base angle  $\theta_d$  of prism changes from  $61.56^\circ$  to  $5^\circ$ . In comparison, changing the base angle of prisms is a relatively more effective method than that of changing the recording wavelength, which has a larger tuning range for the operating wavelength.



(a)

**Figure 8.** Cont.



(b)

**Figure 8.** Relationships of (a) reconstruction wavelength  $\lambda_2$  versus recording wavelength  $\lambda_1$  and diffraction angle  $\theta_d$  versus recording wavelength  $\lambda_1$ ; (b) reconstruction wavelength  $\lambda_2$  versus base angle  $\theta_{p1}$  of right-angle prism.

**Table 1.** Corresponding reconstruction wavelengths and diffraction angles for commercial lasers.

Laser	Recording Wavelength $\lambda_1$ (nm)	Reconstruction Wavelength $\lambda_2$ (nm)	Diffraction Angle $\theta_d$ (°)
He–Cd	441.6	309.7	81.57
Ar+	488.0	342.2	82.29
Ar+	514.5	360.8	82.60
Diode–YAG	532.0	373.1	82.78
He–Ne	632.8	443.6	83.54
Diode	650.0	455.6	83.63

Furthermore, in Figure 6b, combined with camera and analyzer, the characteristic of radial polarization of the HRPC was tested. The captured colorful light field distributions are shown in Figure 9. In Figure 9a–d, both of the transmitting axes of the polarizer and analyzer were set at 0°, 45°, 90°, and 135° with respect to the  $y$ -axis, respectively. The analyzer was added in order to increase the contrast of image. Furthermore, in Figure 9e,f, the transmitting axes of the polarizer and the analyzer were set perpendicular to each other; meanwhile, the transmitting axes of the polarizer were aligned at 0° and 45° with respect to the  $y$ -axis. These results successfully proved the radial polarization characteristic of the holographic radial polarization converter. In Figure 9, the central parts of the light field distributions have strong stray light, which is caused by the uneven intensity of the beam profile of the white-light source. Because the HRPC is operated in a specific narrow band, it is not a problem in practice. In Figure 5, the seam in the prototype is relatively rough. This problem can be easily solved by fine processing during product manufacturing and does not affect the beam quality during use. In addition, with continuously accurate fan-shaped exposures, a HRPC without a seam could be achieved.

Compared with other commercial products and holographic lithography technology [15,16,20], such as space-variant half-wave plates, sub-wavelength metal stripe gratings, liquid-crystal elements, dielectric metasurfaces, and waveguide gratings, the proposed HRPC has the advantage of traditional holographic optical components, such as high diffraction efficiency, thin and compact plane configuration, easy coupling of light, low cost, and suitability for mass production. Due to the design of a large diffraction angle and the application of the prism-hologram-prism sandwiched recording method, the HRPC also has the advantages of easy implementation and a simple recording

process compared to traditional holographic optical components. Listed in Table 2 is the comparison of polarization-selective volume hologram gratings designed at various angles. This design method only needs a small modulated refractive index value to achieve a polarization selection with high diffraction efficiency. For traditional holographic recording materials, such as photopolymers, dichromated gelatin (DCG), and silver-halide gelatin, their limited modulation refractive index cause it difficult to achieve the function of polarization selection under a limited thickness. However, the design of a large diffraction angle can be easily achieved, and the manufacturing method is very easy—only requires one collimated incident beam.

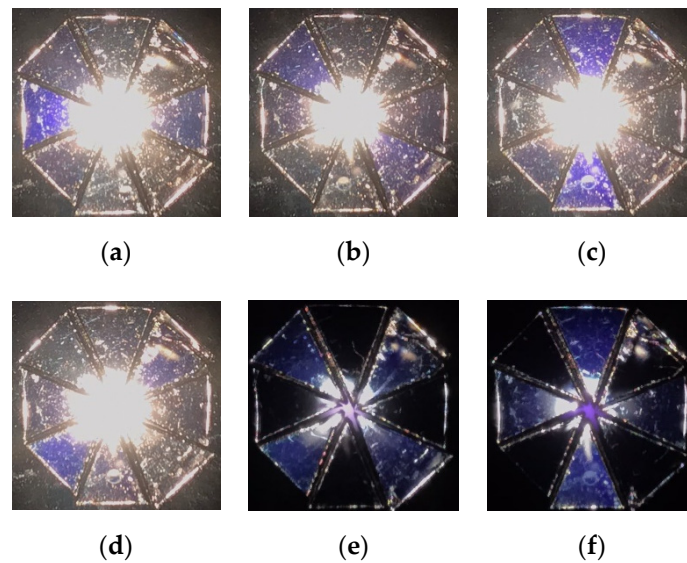


**Figure 9.** Captured light field distributions with both of the transmitting axes of the polarizer and analyzer set at (a) 0°, (b) 45°, (c) 90°, and (d) 135°, and with the transmitting axes of the polarizer set at (e) 0° and (f) 45° with a perpendicular analyzer.

**Table 2.** Comparison of polarization-selective volume hologram gratings designed for various angles.

Design of Polarization-Selective Volume Hologram Gratings						
Diffraction angle, $\theta_d$	48.19°		60°		85°	
Diffraction efficiencies, ( $\eta_s, \eta_p$ )	(100%, 0)		(0, 100%)		(100%, 1.93%)	
Effective index modulation, $N_1 = n_1 d / \lambda_2$	1.22		0.71		0.15	
Maximum refractive index modulation	$n_{DCG} < 0.08$	$n_{SH} < 0.03$ $n_{PP} < 0.03$	$n_{DCG} < 0.08$	$n_{SH} < 0.03$ $n_{PP} < 0.03$	$n_{DCG} < 0.08$	$n_{SH} < 0.03$ $n_{PP} < 0.03$
Satisfied thickness, $d_2 / \lambda_2$	>15.25	>40.67	>8.88	>23.67	>1.88	>5

$n_{DCG}$ : maximum index modulation strength of DCG;  $n_{SH}$ : maximum index modulation strength of silver-halide materials;  $n_{PP}$ : maximum index modulation strength of photopolymers.

#### 4. Conclusions

This research proposed a new design of holographic radial polarization converter with space-variant polarization-selective volume hologram gratings for the first time. The prism-hologram-prism sandwiched holographic recording method was adopted for the recording of PVHGs. A prototype holographic radial polarization converter was successfully assembled and tested. The *s*- and *p*-polarization diffraction efficiencies of the PVHGs at 443.29 nm are 90.83% and 22.09%, respectively. The bandwidth of *s*-polarization light at diffraction efficiency of 80% is about 4.42 nm. The proposed

design should have advantages of most holographic optical elements, meaning that it is especially suitable for low-cost mass production and has high application potential in related fields.

**Author Contributions:** J.-H.C. conceived and designed the experiments; H.-L.T. and F.-H.H. performed the experiments; J.-H.C., C.-Y.H., H.-L.T., and F.-H.H. analyzed the data; J.-H.C., C.-Y.H., K.-H.C., and C.-H.Y., and K.-Y.H. contributed to the materials and provided discussions; J.-H.C. and H.-L.T. wrote the paper. All authors have read and agreed to the published version of the manuscript.

**Funding:** This research was funded by the Ministry of Science and Technology of the Republic of China, grant numbers MOST 107-2221-E-035-069-MY2 and MOST 108-2221-E-239-023.

**Conflicts of Interest:** The authors declare no conflict of interest.

## References

1. Rutkauskas, M.; Farrell, C.; Dorrer, C.; Marshall, K.L.; Lundquist, T.R.; Vedagarbha, P.; Reid, D.T. High-resolution subsurface microscopy of CMOS integrated circuits using radially polarized light. *Opt. Lett.* **2015**, *40*, 5502–5505. [[CrossRef](#)] [[PubMed](#)]
2. Lan, T.-H.; Chung, Y.-K.; Li, J.-E.; Tien, C.-H. Plasmonic rainbow rings induced by white radial polarization. *Opt. Lett.* **2012**, *37*, 1205–1207. [[CrossRef](#)] [[PubMed](#)]
3. Kozawa, Y.; Sato, S. Optical trapping of micrometer-sized dielectric particles by cylindrical vector beams. *Opt. Express* **2010**, *18*, 10828–10833. [[CrossRef](#)] [[PubMed](#)]
4. Meier, M.; Romano, V.; Feurer, T. Material processing with pulsed radially and azimuthally polarized laser radiation. *Appl. Phys. A* **2007**, *86*, 329–334. [[CrossRef](#)]
5. Kiraly, B.; Mannix, A.J.; Jacobberger, R.M.; Fisher, B.L.; Arnold, M.S.; Hersam, M.C.; Guisinger, N.P. Driving chemical interactions at graphene-germanium van der Waals interfaces via thermal annealing. *Appl. Phys. Lett.* **2018**, *113*, 213103. [[CrossRef](#)]
6. Sekkat, Z. Vectorial motion of matter induced by light fueled molecular machines. *OSA Contin.* **2018**, *1*, 668. [[CrossRef](#)]
7. Chang, K.-C.; Lin, T.; Wei, M.-D. Generation of azimuthally and radially polarized off-axis beams with an intracavity large-apex-angle axicon. *Opt. Express*. **2013**, *21*, 16035–16042. [[CrossRef](#)] [[PubMed](#)]
8. Bomzon, Z.; Kleiner, V.; Hasman, E. Formation of radially and azimuthally polarized light using space-variant subwavelength metal stripe gratings. *Appl. Phys. Lett.* **2001**, *79*, 1587–1589. [[CrossRef](#)]
9. Han, C.-Y.; Chang, R.-S.; Chen, H.-F. Solid-state interferometry of a pentaprism for generating cylindrical vector beam. *Opt. Rev.* **2013**, *20*, 189–192. [[CrossRef](#)]
10. Nicolas, P.; de Renaud, S.D.; Kamel, A.-A.; François, T.; Rolland, H.; Roch, J.-F. Simple interferometric technique for generation of a radially polarized light beam. *J. Opt. Soc. Am. A* **2005**, *22*, 984–991.
11. Han, C.-Y.; Wei, Z.-H.; Hsu, Y.; Chen, K.-H.; Yeh, C.-H.; Wu, W.-X.; Chen, J.-H. Generating Radially and Azimuthally Polarized Beams by Using a Pair of Lateral Displacement Beamsplitters. *Appl. Sci.* **2016**, *6*, 241. [[CrossRef](#)]
12. Lerman, G.M.; Levy, U. Generation of a radially polarized light beam using space-variant subwavelength gratings at 1064 nm. *Opt. Lett.* **2008**, *33*, 2782–2784. [[CrossRef](#)] [[PubMed](#)]
13. Jourlin, Y.; Tonchev, S.; Parriaux, O.; Sauvage-Vincent, J.; Harzendorf, T.; Zeitner, U. Waveguide Grating Radial Polarizer for the Photolithography of Circularly Symmetrical Optical Elements. *IEEE Photonics J.* **2012**, *4*, 1728–1736. [[CrossRef](#)]
14. Mao, H.; Chen, Y.; Liang, C.; Chen, L.; Cai, Y.; Ponomarenko, S.A. Self-steering partially coherent vector beams. *Opt. Express* **2019**, *27*, 14353–14368. [[CrossRef](#)] [[PubMed](#)]
15. Arbabi, A.; Horie, Y.; Bagheri, M.; Faraon, A. Dielectric Metasurfaces for Complete Control of Phase and Polarization with Subwavelength Spatial Resolution and High Transmission. *Nat. Nanotechnol.* **2015**, *10*, 937–943. [[CrossRef](#)] [[PubMed](#)]
16. Luo, J.; Zhang, Z.; Song, M.; He, A.; Yu, H. Simultaneous generation and focus of radially polarized light with metal-dielectric grating metasurface. *Opt. Commun.* **2017**, *382*, 421–427. [[CrossRef](#)]
17. Huang, Y.-T. Polarization-selective volume holograms: General design. *Appl. Opt.* **1994**, *33*, 2115–2120. [[CrossRef](#)] [[PubMed](#)]

18. Hsu, F.-H.; Han, C.-Y.; Chen, K.-H.; Hsu, K.-Y.; Chen, J.-H. Prism-hologram-prism sandwiched recording method for polarization-selective substrate-mode volume holograms with a large diffraction angle. *Opt. Express* **2018**, *26*, 20534–20543. [[CrossRef](#)] [[PubMed](#)]
19. Kogelnik, H. Coupled wave theory for thick hologram gratings. *Bell Syst. Tech. J.* **1969**, *48*, 2909–2947. [[CrossRef](#)]
20. Lin, J.; Genevet, P.; Kats, M.A.; Antoniou, N.; Capasso, F. Nanostructured Holograms for Broadband Manipulation of Vector Beams. *Nano Lett.* **2013**, *13*, 4269–4274. [[CrossRef](#)] [[PubMed](#)]



© 2020 by the authors. Licensee MDPI, Basel, Switzerland. This article is an open access article distributed under the terms and conditions of the Creative Commons Attribution (CC BY) license (<http://creativecommons.org/licenses/by/4.0/>).